ISSN 1063-7834, Physics of the Solid State, 2017, Vol. 59, No. 6, pp. 1118–1126. © Pleiades Publishing, Ltd., 2017.
Original Russian Text © V.S. Bondarev, E.A. Mikhaleva, I.N. Flerov, M.V. Gorev, 2017, published in Fizika Tverdogo Tela, 2017, Vol. 59, No. 6, pp. 1097–1105.

FERROELECTRICITY

Electrocaloric Effect in Triglycine Sulfate under Equilibrium and Nonequilibrium Thermodynamic Conditions

V. S. Bondarev[a,b,*], E. A. Mikhaleva[a], I. N. Flerov[a,b], and M. V. Gorev[a,b]

[a] *Kirensky Institute of Physics, Federal Research Center "Krasnoyarsk Science Center," Siberian Branch, Russian Academy of Sciences, Krasnoyarsk, 660036 Russia*

[b] *Siberian Federal University, Krasnoyarsk, 660041 Russia*

**e-mail: vbondarev@yandex.ru*

Received November 22, 2016

Abstract—The direct and indirect measurements of intensive electrocaloric effect in a triglycine sulfate ferroelectric crystal are performed under equilibrium and nonequilibrium thermodynamic conditions implemented in the adiabatic calorimeter. The effect of the electric field parameters (frequency, profile, and strength) on the value of the effect and degree of its reversibility are studied. The difference between the temperature variation values in a switched-on and switched-off dc field under quasi-isothermal conditions is established. The low-frequency periodic electric field induces the temperature gradient along the electrocaloric element and heat flux from its free end to the thermostated base. A significant excess of the field switching-off rate over the switching-on rate leads to a noticeable intensification of the cooling effect.

DOI: 10.1134/S1063783417060051

1. INTODUCTION

One of the promising directions in searching for new cooling techniques and creating refrigerating devices, which have been intensively developed in recent years by scientists and engineers, is the study of various caloric effects (CEs) in solids [1–8]. Such phenomena are based on the principle of reversible temperature variation ΔT_{AD} or entropy variation ΔS_{CE} in a solid under the action of an external field (electric, magnetic, or mechanical stress) under adiabatic or isothermal conditions [1, 4, 8]. The external field changes the temperature dependence of the corresponding order parameter (polarization, magnetization, and strain), which, in turn, causes cooling/heating of a solid element (cooling agent). The consistent periodic variation in the strength of a field applied to the working element and in the conditions for thermodynamic conjugation of the cooling agent with the environment makes it possible to perform a closed cooling cycle. Since the most significant temperature variations in the order parameter and its susceptibility to the field change are observed in the region of phase transitions, the CE attains its maximum values in this temperature range. This explains the enhanced interest of research in the materials undergoing electrical, magnetic, or elastic phase transitions.

Owing to the high density of solids, cooling devices based on them can be essentially compact as compared with the traditional vapor-liquid refrigerators. Thus, the use of solid cooling agents in refrigerating devices is both reasonable and preferable.

From the engineering viewpoint, the electrocaloric effect (ECE) is easier to implement than the magnetocaloric (MCE) and barocaloric (BCE) effects, since it is sufficient to apply voltage to electrodes deposited onto opposite sides of a crystal or ceramic element. This is one of the reasons for the increased number of recent studies and publications devoted to the ECE [3, 4, 9, 10]. One of the main goals of these works is the search for the ways of creating and improving the well-known materials to attain large absolute values of the intensive (ΔT_{AD}) and extensive (ΔS_{ECE}) effects. However, in this case, high electric field strengths E are required, which often lead to the electrical breakdown of bulk electrocaloric (EC) elements [11]. They try to solve the latter problem using film ferroelectric elements, in which large E values can be attained at low voltages [12, 13]. This allows obtaining encouraging results on enhancing the intensive ECE, which are similar to the best results obtained in ferromagnets due to the MCE [2, 8]. However, in virtue of insignificant volume (mass) of the film elements, the extensive ECE appears too weak to speak about their application potential.

Taking into account the aforementioned problems typical of ferroelectric caloric elements studied and planned for application under equilibrium thermal and electrical conditions, it seems very promising to employ the hypothetic possibility of significant ECE

enhancement by applying a periodic field to solids that are under nonequilibrium thermal conditions. This problem has been recently theoretically solved for ferroelectrics with the high dielectric susceptibility χ and significantly nonlinear derivative $\partial\chi/\partial T$ [14–16]. The periodic field E affecting a sample with one thermostated edge induces the temperature gradient, dynamic polarization, and heat flux. In the paraelectric phase, the amount of absorbed heat is larger than the amount of the released heat, which causes cooling of an element under nonequilibrium thermal conditions.

Recently, we have experimentally investigated the ECE induced by ac field E in a ferroelectric element in the form of a four-face rectangular prism from the triglycine sulfate crystal (TGS) [17]. The most important technological task was to keep a constant temperature of the prism base. The measurements were performed in a moderate vacuum (a residual pressure of 10^{-2} mmHg) without additional measures to exclude heat exchange between the sample and environment. As a result, we observed cooling of the caloric element, which depended, as was expected in [14–16], on the E frequency. However, the temperature difference between the thermostated base and free end of the EC element was found to be much smaller than its value calculated with regard to the experimental conditions [17]. The weak effect of the TGS element cooling was attributed to the heat exchange with the environment, poor heat contact between the temperature sensor and EC element, and the observed conductivity of the investigated sample. Many of the above-listed factors can be eliminated or weakened by performing the measurements under adiabatic conditions. From this viewpoint, the method most suitable for studying the intensive ECE is the adiabatic calorimeter. It is characterized by the high sensitivity to minor temperature variation ΔT_{AD} and, in addition, makes it possible to determine the extensive ΔS_{ECE} effect by measuring and analyzing specific heat as a function of the electric field strength.

In this study, we continue to investigate the ECE in the TGS ferroelectric crystal under equilibrium and nonequilibrium conditions. All the experiments were conducted in an adiabatic calorimeter with a system of heat screens, which best exclude the heat exchange between the sample and environment [18]. Direct and indirect investigations of the ECE upon variation in the electric field parameters were carried out.

2. EXPERIMENTAL

The investigations were carried out using samples fabricated from the bulk TGS single crystal grown in the paraelectric phase from the aqueous solution under the maximally equilibrium thermal conditions, which was used by us in [17] to study the ECE. Powder X-ray diffraction (XRD) patterns showed no reflections of foreign phases and impurities in the crystal. The temperature $T_C = 322.37$ K of the phase transition $P2_1/m \leftrightarrow P2_1$, the maximum permittivity $\varepsilon_b^{max} = 3 \times 10^4$, and the polarization $P = 2.5$ μC cm^{-2} at 290 K, and the polarization behavior determined in [17] are in satisfactory agreement with the results of previous investigations [19, 20].

A specific feature of the CE, in particular, the ECE, is that only the intensive (ΔT_{AD}) effect can be measured directly. The extensive (ΔS_{CE}) effect is determined by indirect techniques. According to the analysis and comparative estimation of different methods for studying the ECE [21], both approaches, direct and indirect, can be used, but, certainly, direct measurements of ΔT_{AD} are preferable.

The essence of the intensive ECE is such that its real value should be determined upon switching on/off the electric field at the constant entropy of the investigated sample. On the other hand, one of the ways of obtaining information about the extensive ECE is to analyze data on the temperature dependences of specific heat at $E = 0$ and $E \neq 0$. The optimal method for solving these problems simultaneously is an adiabatic calorimeter. In addition, as we demonstrate below, such a calorimeter allows determining the intensive ECE under nonequilibrium conditions and varied electric field frequency.

The calorimetric setup used in this study is analogous to that described in [18]. Here, we present only the features of sample mounting and the construction of a measuring cell (Fig. 1).

All the investigations were carried out on one TGS sample (*1*) in the form of rectangular parallelepiped ($10 \times 6 \times 1$) mm^3 (Fig. 1a). Gold electrodes *2* were formed by vacuum deposition on the EC element faces with the largest area, which are perpendicular to the ferroelectric *b* axis. The voltage applied to the elec-

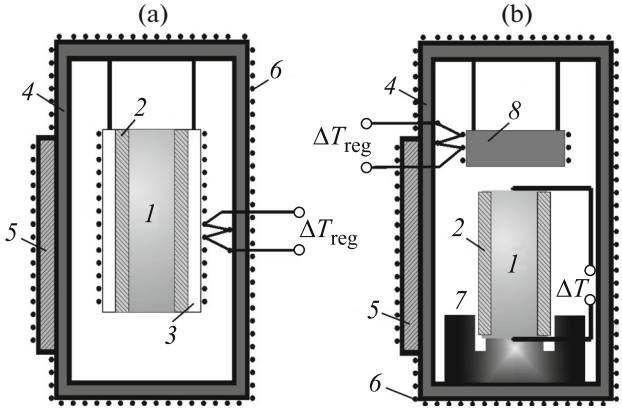

Fig. 1. Schematic of sample mounting for studying (a) the specific heat and ECE under adiabatic conditions and (b) the effect of quasi-isothermal processes of switching on/off the dc and periodic electric fields.

trodes induced electric field E inside the sample. To prevent electric breakdown, thin (~0.2 mm) mica plates *3* were glued on the top of the electrodes. The prepared sample was packed in a polished aluminum foil with the glued heater. The reliable heat contact between the elements of the system sample + hardware (mica + foil with the heater) was ensured using a vacuum lubricant.

To measure the ECE and specific heat under equilibrium conditions, the system was hung on thin threads ($d \le 0.1$ mm) inside the adiabatic screen *4* of the calorimeter (Fig. 1a). The sample temperature was controlled with a precision platinum resistance thermometer *5* mounted on the adiabatic screen. The temperature difference ΔT_{reg} between the adiabatic screen and sample was controlled and tuned using a copper-constantan thermocouple battery, the signal from which was supplied to the circuit of a precision power amplifier connected to adiabatic screen heater *6*. The radiation and convective heat exchange were minimized by additional screens and by placing the entire measuring system in a high-vacuum (~10^{-5} mmHg) envelope [18].

The relaxation study of the intensive ECE under nonequilibrium thermal conditions was carried out in the following manner (Fig. 1b). The TGS sample base with electrodes *1* was placed in a copper holder *7* mounted on an adiabatic screen *4*. A copper disk *8* with $d = 7.94$ mm and $h = 1.89$ mm packed in the polished aluminum foil with a heater and serving as an additional heat screen was hung over the sample to the screen cover. A reliable heat contact between all system elements was ensured by using a vacuum lubricant. The automated control system retained the required temperature difference between the copper disk and adiabatic screen with an accuracy of no worse than 10^{-4} K. Thus, the constant temperature of the adiabatic screen was kept and, thus, the isothermal conditions T_{bot} = const were established for the TGS sample base. The temperature difference $T_{top} - T_{bot}$ between the top free end and the bottom thermostated end of the sample, which occurred due to the ECE at the switching-on/off field E was detected by the copper-constantan thermocouple. The sensitivity of the temperature sensors and measurement stability were 10^{-4} and 5×10^{-4} K, respectively.

3. RESULTS AND DISCUSSION

3.1. Study of the effect of the electric field on specific heat. At the first stage, we studied the effect of the electric field on specific heat $C(T, E)$ of the TGS sample by the traditional adiabatic calorimeter method. The measurements were performed in the temperature range of 270–335 K by discrete and continuous heating at rates of $dT/dt = 2.3$ K h^{-1} and $dT/dt = 0.2$ K min^{-1}. The hardware specific heat measured in a separate experiment was ~50% of the total specific heat of the system sample + hardware.

Since we analyzed the ECE near the phase transition temperature, Fig. 2a shows the $C(T, E)$ dependences in a narrow temperature range at electric field strengths of 0–2.8 kV cm^{-1}. At $E = 0$, the specific heat anomaly corresponding to the ferroelectric–paraelectric phase transition was observed at $T_C = 322.25 \pm 0.05$ K, which agrees well with the data obtained in [17, 19]. The behavior of specific heat in a field corresponds to that observed previously in [19], i.e., to a decrease in the maximum and spread of the specific heat jump.

To obtain information about the anomalous entropy $\Delta S_{an}(T, E) = \int [\Delta C_{an}(T, E)/T] dT$ related to the phase transition, we had to separate the lattice specific heat $C_L(T)$ independent of E and the anomalous specific heat $\Delta C_{an}(T, E)$. The lattice contribution was determined by approximation of the total specific heat far from the phase transition temperature using the Debye and Einstein function combination. The behavior of the anomalous entropy upon temperature and electric field strength variation is illustrated in Fig. 2b.

The temperature dependences of the extensive ECE at different electric field strengths determined as a difference between the entropies at $E \neq 0$ and $E = 0$

$$\begin{aligned} \Delta S_{ECE}(T, E) &= S(T, E) - S(T, 0) \\ &= \Delta S_{an}(T, E) - \Delta S_{an}(T, 0), \end{aligned} \quad (1)$$

are presented in Fig. 2c.

The intensive ECE $\Delta T_{AD}(T, E)$ was determined from the data on the total sample entropy $S(T, E)$ in accordance with the condition

$$S(T, E) = S(T + \Delta T_{AD}, 0). \quad (2)$$

The maximum values of $\Delta S_{ESE}^{max} = -0.329$ J (mol K)$^{-1}$ and $\Delta T_{AD}^{max} = 0.198$ K at $E = 2.8$ kV cm^{-1} were observed at $T_{ECE}^{max} = 322.54 \pm 0.05$ K, i.e., above the phase transition temperature T_C at $E = 0$. The difference between these temperatures is caused by the fact that T_C corresponds to the maximum anomalous specific heat related to the temperature derivative of squared polarization $\Delta C_{an}^{max} \sim (\partial \Delta S_{an}/\partial T)^{max} \sim (\partial P^2/\partial T)^{max}$ [22] and T_{ECE}^{max} is determined by the relation $\Delta S_{ESE}^{max} \sim \Delta T_{AD}^{max} \sim (\partial P/\partial T)^{max}$ [4].

3.2. Direct measurements of the intensive ECE under adiabatic conditions. The classical experiment on the direct determination of the intensive ECE under adiabatic conditions in accordance with a scheme presented in Fig. 1a included several sequential stages (Fig. 3a). The system sample + hardware was heated/cooled to the temperature at which further investigations were carried out and a linear tempera-

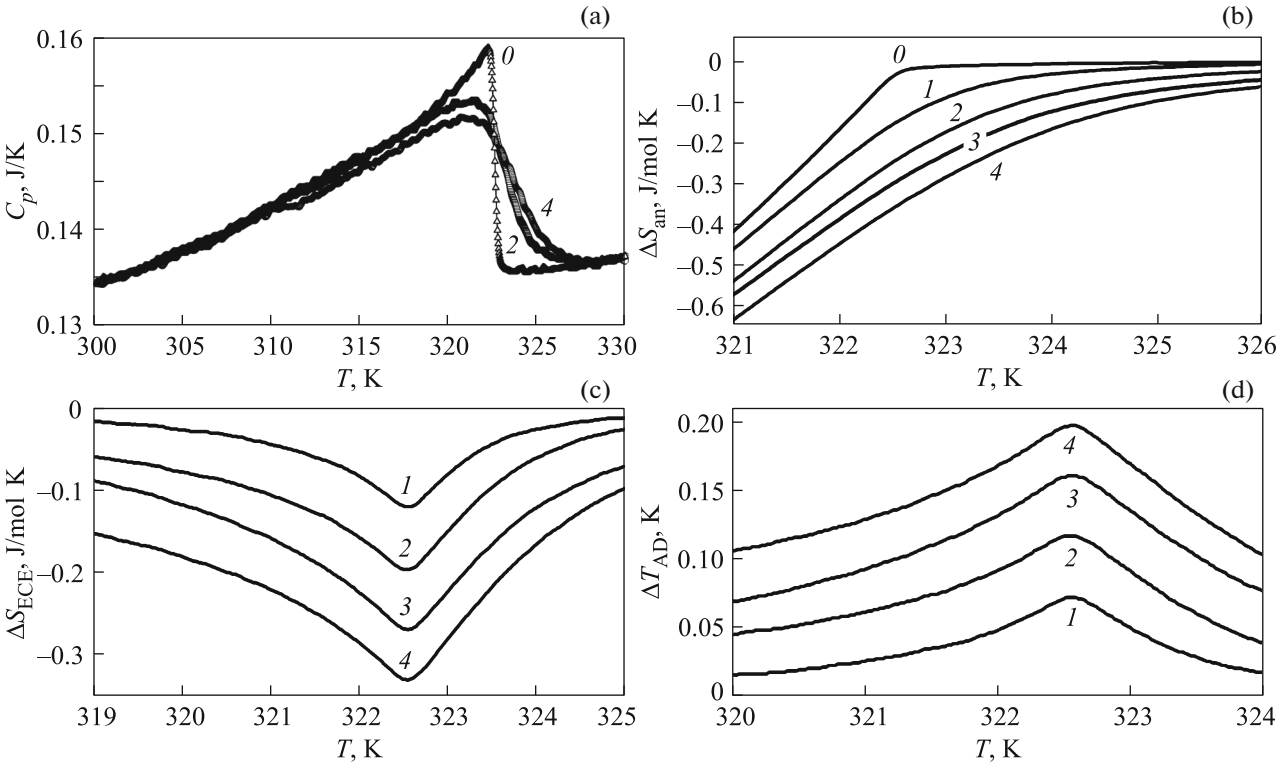

Fig. 2. Temperature dependences of (a) specific heat of the system sample + hardware in dc fields, (b) TGS anomalous entropy $\Delta S_{an}(T, E)$, (c) extensive ΔS_{ECE}, and (d) intensive ΔT_{AD}. The numbers of the curves correspond to strengths E of (*0*) 0, (*1*) 0.7, (*2*) 1.4, (*3*) 2.1, and (*4*) 2.8 kV cm^{-1}.

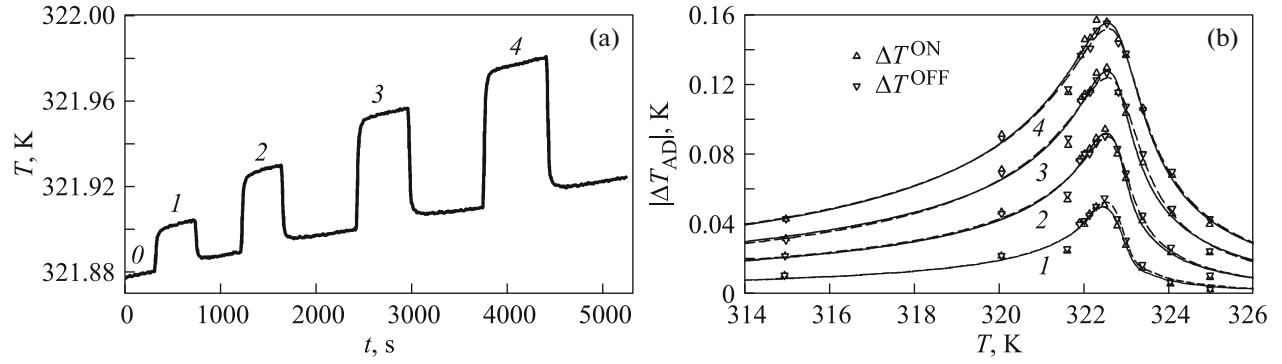

Fig. 3. (a) Dependence of the temperature of the system sample + hardware on electric field strengths of (*0*) 0, (*1*) 0.7, (*2*) 1.4, (*3*) 2.1, and (*4*) 2.8 kV cm^{-1}. (b) Temperature dependences of the intensive ECE determined from (3) for the switching on (ΔT_{AD}^{ON}) and switching off (ΔT_{AD}^{OFF}) the electric field.

ture drift at an optimal rate was specified within $dT/dt \approx \pm(1–5) \times 10^{-4}$ K min^{-1}. Then, a voltage pulse with a length of 5–10 min was supplied to the sample electrodes, which led, due to the ECE, to the sharp growth of the system temperature by a value of ΔT_{exp}^{ON}, which is lower than ΔT_{AD} due to the heat loss to heating the passive system elements (mica, heater, and lubricant). After switching off the field, the sample temperature sharply decreased by a value of ΔT_{exp}^{OFF}. Then, the process was repeated at the electric field strength (Fig. 3a). The error of determination of the ΔT_{exp} was no more than $\pm 2 \times 10^{-4}$ K.

A minor temperature variation in each experiment (Fig. 3a) by the expense of a very small temperature

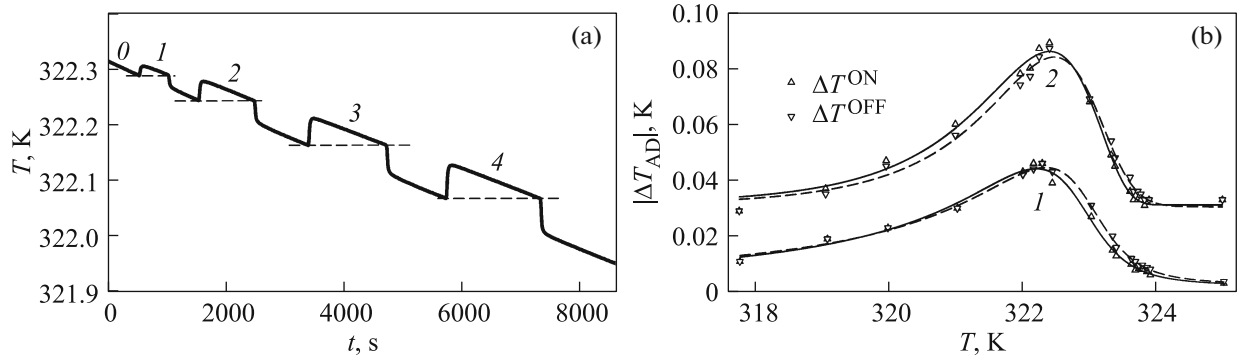

Fig. 4. (a) ECE in the TGS crystal under quasi-isothermal conditions. (b) Measured ΔT_{exp} values with a gradual increase in E. Temperature dependences of ΔT_{AD} near the phase transition. The numbers of the curves correspond to strengths E of (*0*) 0, (*1*) 0.7, (*2*) 1.4, (*3*) 2.1, and (*4*) 2.8 kV cm^{-1}.

drift $dT/dt \approx 3.3 \times 10^{-4}$ K min^{-1} at $E = 0$ ensured the adiabatic conditions. At $E \neq 0$, the system temperature variation rate after the transition period should not be different from $(dT/dt)_{E=0}$. However, in the experiment, it appeared much larger and attained $dT/dt \approx 6.8 \times 10^{-4}$ K min^{-1} at $E = 2.8$ kV cm^{-1}. This evidences for the presence of conductivity in the investigated TGS crystal near the phase transition, which leads to the Joule heat release on the sample resistance at $E \neq 0$. The noticeable conductivity of the TGS crystal resulted in the situation that after switching off the electric field, the sample temperature did not return to the expected level corresponding to the extrapolation of the previous temperature path (Fig. 3a). The ΔT_{exp} value was determined as a difference between temperatures obtained by the linear extrapolation of the $T(t)$ dependences by the moment of switching on/off or off the field.

To determine the real ΔT_{AD} value, it is necessary to correct the experimental ΔT_{exp} value, since the heat released by the ECE is spent to the variation in both the sample temperature and the temperature of the entire system sample + hardware. The relation between the ΔT_{exp} and ΔT_{AD} values is

$$\Delta T_{AD} = \Delta T_{exp}\left(1 + \frac{C_f}{C_{smp}}\right), \quad (3)$$

where C_f is the hardware specific heat determined in a separate experiment and C_{smp} is the sample specific heat.

Figure 3b presents temperature dependences of the intensive ECE corrected in accordance with (3) at switching on (ΔT_{AD}^{ON}) and switching off (ΔT_{AD}^{OFF}) the electric field. At $E = 2.8$ kV cm^{-1}, the intensive ECE attains the maximum value of $|\Delta T_{AD}|^{max} = 0.154$ K at a temperature of 322.53 ± 0.05 K coinciding with the value of $T_{ECE}^{max} = 322.54$ K determined from the $S(T, E)$ dependences. However, the $|\Delta T_{AD}|^{max}$ values obtained in the direct measurements appeared smaller than the values calculated at the same strengths $\boldsymbol{E}$ (Fig. 2d) within 20%. This discrepancy between the ΔT_{AD} values determined by the direct and indirect methods is often met for the CE of different natures [21, 23].

The temperature variation after switching on the electric field of different strengths ΔT_{AD}^{ON} coincided with the ΔT_{AD}^{OFF} value within a few percent. For instance, at $E = 2.8$ kV cm^{-1} and $T = 323.0$ K, these values were +0.136 and −0.137 K. The data obtained by multiple measurements are indicative of the high degree of reproducibility and reversibility of the intensive ECE in the TGS crystal under adiabatic conditions and agree quite satisfactorily with the data obtained earlier for only the ΔT_{AD}^{ON} value [24].

It should be noted that in our experiments switching on and off the field E was performed at slightly different temperatures, specifically, at T and $T + \Delta T_{AD}$ (Fig. 3a). In addition, we performed the ECE measurements at switching on and off the field E at the same temperature (Fig. 4a): $(T, E = 0) \rightarrow (T + \Delta T_{AD}^{ON}, E \neq 0)$ and $(T, E \neq 0) \rightarrow (T - \Delta T_{AD}^{OFF}, E = 0)$. For this purpose, we specified a negative rate of the variation in the temperature of the system sample + hardware, the absolute value of which, $dT/dt = -2.5 \times 10^{-3}$ K/min, was larger than the rate in the experiments with $dT/dt > 0$ by an order of magnitude (Fig. 3a). A sufficiently high cooling rate of the system at $E = 0$ was necessary to attain in the process with $E \neq 0$ the temperature of switching on the field for 10–30 min. Some results of such experiments are illustrated in Fig. 4b.

We observed the difference between the ΔT_{AD}^{ON} and ΔT_{AD}^{OFF} values, which is larger than the measurement error and have different signs in the ferroelectric ($|\Delta T_{AD}|^{ON}(T, E) > |\Delta T_{AD}|^{OFF}(T, E)$ and paraelectric ($|\Delta T_{AD}|^{ON}(T, E) < |\Delta T_{AD}|^{OFF}(T, E)$ phases. In particu-

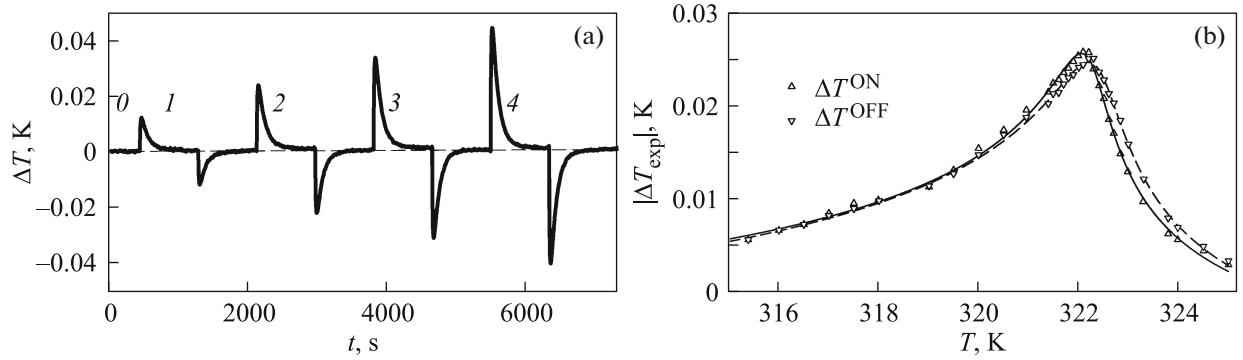

Fig. 5. (a) ECE in the TGS crystal under quasi-isothermal conditions at T_{bot} = 322.3 K. (b) Measured T_{exp} values with a gradual increase in E. Temperature dependences of $|\Delta T_{exp}|$ near the phase transition at E = 1.4 kV cm^{-1}. The numbers of the curves correspond to strengths of (*0*) 0, (*1*) 0.7, (*2*) 1.4, (*3*) 2.1, and (*4*) 2.8 kV cm^{-1}.

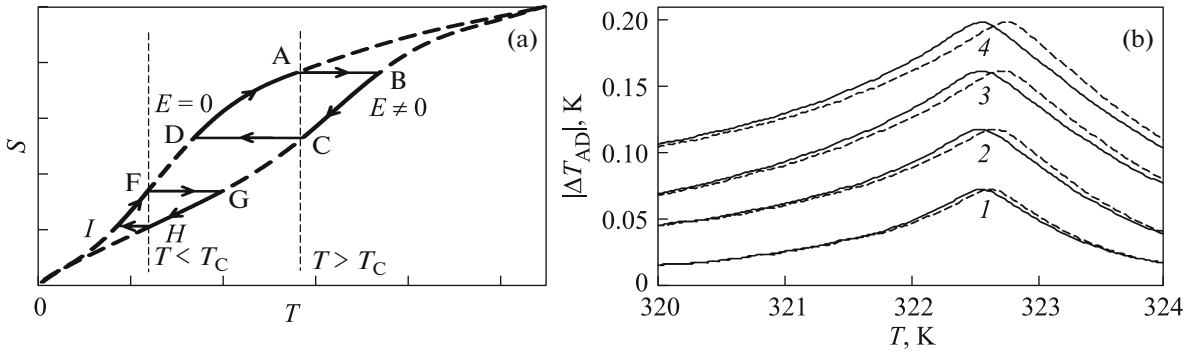

Fig. 6. (a) Cycles of the conditional S–T diagram consisting of the processes of switching on/off the field E at S = const and temperature relaxation at E = const: ABCD—$T > T_C$ and FGHI—$T < T_C$. (b) Temperature dependences of $|\Delta T_{AD}|^{ON}$ (solid lines) and $|\Delta T_{AD}|^{OFF}$ (dashed lines) determined from the TGS S–T diagram. The numbers of the curves correspond to strengths of 0, (*1*) 0.7, (*2*) 1.4, (*3*) 2.1, and (*4*) 2.8 kV cm^{-1}.

lar, the field E = 1.4 kV cm^{-1} leads to the following effects: at T = 321 K < T_C, ΔT_{AD}^{ON} = 0.060 K and ΔT_{AD}^{OFF} = –0.056 K and at T = 323.5 K > T_C, ΔT_{AD}^{ON} = 0.046 K and ΔT_{AD}^{OFF} = –0.050 K.

3.3. Study of the intensive ECE by the relaxation technique under quasi-isothermal conditions. Study of the ECE by the relaxation technique was carried out on the TGS sample mounted according to the scheme shown in Fig. 1b. These conditions are quasi-isothermal, since during the measurements only the temperature T_{bot} of the sample bottom was kept constant. At the fast (adiabatic) switching on/off the electric field, the temperature of the top free sample end rapidly grew/dropped due to the ECE and then, at E = const, relaxed fairly slowly to the value corresponding to the temperature T_{bot} (Fig. 5a).

The temperature gradient occurring on the sample led to the heat exchange between the bottom (thermostated) and top (thermodynamically free) ends of the EC element. If the $|\Delta T_{exp}|^{ON}$ and $|\Delta T_{exp}|^{OFF}$ values are analogous, then the amounts of heat transferred in the directions $T_{top} \rightarrow T_{bot}$ and $T_{bop} \rightarrow T_{top}$, respectively, are equivalent as well. In this case, the resulting effect of sample cooling is absent. However, the experimental data show (Fig. 5b) that the $|\Delta T_{exp}|^{ON}$ and $|\Delta T_{exp}|^{OFF}$ values are unequal. It should be noted that, in this case, the correction of $|\Delta T_{exp}|$ according to (3) was not performed, since it was difficult to reliably estimate the specific heat C_f, which, judging by the ratio between $|\Delta T_{exp}|$ (Fig. 5b) and $|\Delta T_{AD}|$ (Fig. 4b), is several times higher than C_{smp} in the relaxation technique for measurements under quasi-isothermal conditions. The most important point is that the ratios between the intensive ECE in the considered case (Fig. 5b) were the same as in the experiments conducted under adiabatic conditions with $dT/dt < 0$ (Fig. 4), specifically, at $T < T_C$, $|\Delta T_{exp}|^{ON} > |\Delta T_{exp}|^{OFF}$ and, at $T > T_C$, $|\Delta T_{exp}|^{ON} < |\Delta T_{exp}|^{OFF}$. The results obtained by the discussed relaxation measurements can be explained using the S–T diagram, which presents the behavior of the total

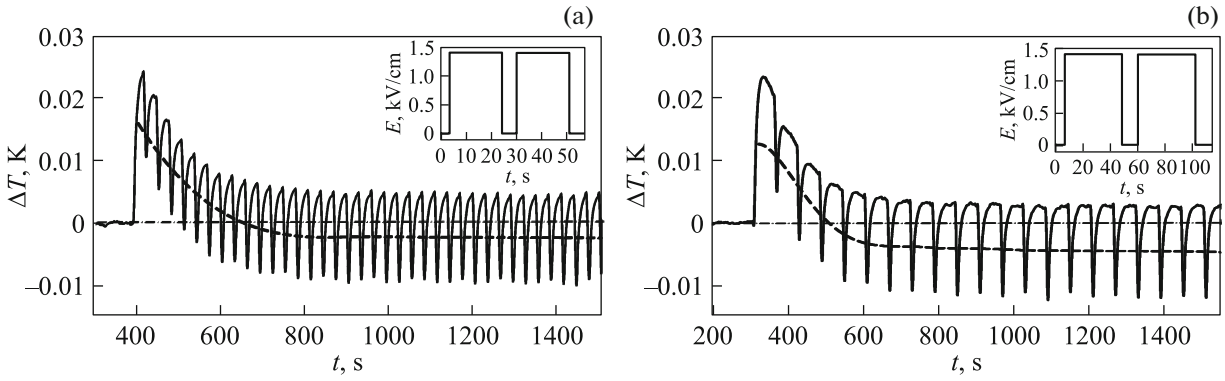

Fig. 7. Time dependence of the temperature difference $\Delta T = T_{top} - T_{bot}$ on the EC element in a periodic electric field of $E = 1.4$ kV cm^{-1} at 322.35 K: (a) $f = 0.036$ and (b) 0.018 Hz. Solid lines show the difference between the T_{top} and constant T_{bot} values. Insets: electric field profile.

entropy of a hypothetic EC element in the vicinity of the phase transition at $E = 0$ and $E \neq 0$ (Fig. 6a).

The ABCD ($T > T_C$) and FGHI ($T < T_C$) cycles consisting of two adiabatic and two isofield processes clearly demonstrate the experimentally observed ratios between the ΔT_{AD}^{ON} and ΔT_{AD}^{OFF} values.

Using the relaxation approach, we can also analyze the ECE data obtained in the investigations of the specific heat $C(T, E)$ (Fig. 2). In this case, we also observed the discrepancy between the ΔT_{AD}^{ON} and ΔT_{AD}^{OFF} values above and below T_C (Fig. 6b). The differences $|\Delta T_{AD}|^{OFF} - |\Delta T_{AD}|^{ON}$ obtained in three independent experiments in the paraelectric phase at $T =$ 323.6 K were found to be similar: 3.5×10^{-3} K (Fig. 4b), 2.7×10^{-3} K (Fig. 5b), and 3×10^{-3} K (Fig. 6b).

The coincidence of the data obtained under different conditions for conjugation of the ECE element with the environment undoubtedly provides evidence of their high reliability.

3.4. Study of the ECE in a periodic electric field. The data shown in Fig. 5 can be characterized as obtained in a periodic electric field with a very low frequency (~6×10^{-4} Hz) and amplitude E increasing in the beginning of each period. At the next stage, we studied the effect of the frequency of field E on the value and character of T_{top} of the sample at $T_{bot} =$ const. In contrast to the analogous measurements performed by us previously in low vacuum (~10^{-2} mmHg) [17], the considered experiments in the adiabatic calorimeter at a pressure of ~10^{-5} mmHg and frequencies of 0.036 and 0.018 Hz appeared possible only at $E \leq$ 1.4 kV cm^{-1}.

In accordance with the results of [17], we chose a rectangular signal profile (Fig. 7) with a filling factor of 85%. Study of the ECE under such electric conditions showed that the stationary state of the system was attained after 10–20 pulses. As a result, the average temperature difference $(\Delta T^{ON} + \Delta T^{OFF})/2$ between the free end and thermostated base of the EC element became negative, oscillating within $\pm(7–8) \times 10^{-3}$ K (Figs. 7a and 7b). The electric pulse repetition rate affected fairly strong the degree of cooling of the EC element. In particular, at $f = 0.036$ Hz, the maximum average temperature difference is $[(\Delta T^{ON} + \Delta T^{OFF})/2]_{max} = 0.0027$ K and, at $f = 0.018$ Hz, attains 0.0050 K. Taking into account the oscillation amplitude, the lowest temperature of the sample free end is $T_{top} = T_{bot} - 0.012$ K.

At first glance, comparison with the data obtained in low vacuum ($[(\Delta T^{ON} + \Delta T^{OFF})/2]_{max} \approx -0.02$ K) [17] does not provide evidence for the aforementioned results. However, it should be taken into account that in [17] the measurements were performed at lower frequencies and higher strengths E.

All the experiments considered above on the determination of the ECE in TGS were conducted at high and equal rates of switching on/off the electric field, which allow us to speak about the adiabatic character of the corresponding processes. Recently, the so-called kinetic ECE in the multilayer $BaTiO_3$ ferroelectric was studied [25]. The experiments were conducted in a differential scanning calorimeter, which allows measuring the amount of heat released/absorbed upon switching on/off the electric field under isothermal conditions. The originality of the study consisted in the fact that the authors used significantly different field variation rates dE/dt: 1.4 kV (cm s)$^{-1}$ in the process $0 \rightarrow E_{max}$ and 176 kV (cm s)$^{-1}$ at $E_{max} \rightarrow 0$. This led to the situation when only in the second case the significant endothermic effect was observed in a narrow time interval due to the adiabatic (fast) elimination of the field.

Using the same technique, we studied the effect of unbalanced rates of the processes $0 \rightarrow E_{max}$ and $E_{max} \rightarrow$

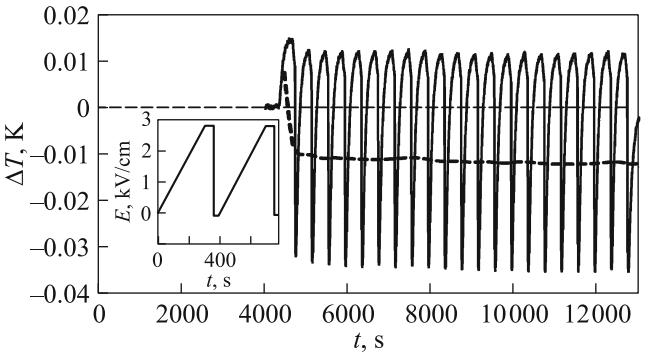

Fig. 8. Time dependence of the temperature difference $\Delta T = T_{top} - T_{bot}$ at 322.545 K in a periodic electric field of $E = 2.8$ kV cm^{-1}, $f = 0.0025$ Hz. The solid line shows the difference between the mean T_{top} and constant T_{bot} values. Insets: electric field profile.

0 on the ECE in TGS. We established the optimal signal shape and electric field frequency, which allowed the more significant cooling parameters to be obtained (Fig. 8).

For an electric field of $E = 2.8$ kV cm^{-1} and $f = 0.0025$ Hz at a filling factor of 93%, the largest average temperature difference attained a more significant value of $[(\Delta T^{ON} + \Delta T^{OFF})/2]_{max} = -0.012$ K than in the measurements at the rectangular E profile. In this case, the lowest temperature of the free end of the EC element was lower than T_{bot} by ~0.035 K.

4. CONCLUSIONS

Using the adiabatic calorimeter technique, we studied the intensive ECE ΔT_{AD} in the region of the ferroelectric phase transition in the TGS crystal. We investigated some aspects of the effect of equilibrium and nonequilibrium (adiabatic and quasi-isothermal) conditions of conjugation of the EC element with the environment and electric field parameters on the value and degree of reversibility of ΔT_{AD} and established the following important facts:

1. The results of direct ECE measurements under adiabatic conditions upon switching on/off the field at different temperatures T and $T + \Delta T_{AD}$ demonstrate the high degree of reproducibility and reversibility of the ΔT_{AD}^{ON} and ΔT_{AD}^{OFF} values. A discrepancy of ~20% between the ΔT_{AD} values measured directly and determined from the S–T diagram based on the obtained data on the effect of the electric field on the TGS specific heat is no surprise, taking into account the analysis made in [21]. The experimentally observed conductivity of the TGS crystal results in the Joule heat release on the sample resistance at $E \neq 0$ and the irreversible contribution to its temperature variation.

2. We investigated the effect of the nonequilibrium process $E = \text{const}$ on the ECE, when the temperature of the EC element lowers $(T + \Delta T_{AD}) \rightarrow T$; i.e., the electric field is switched on/off at the same temperature (Figs. 4a, 5a, and 6a). The satisfactorily agreed results of three independent experiments indicate the discrepancy between the ΔT_{AD}^{ON} and ΔT_{AD}^{OFF} values and their different ratios in the ferroelectric phase $|\Delta T_{AD}|^{ON}(T, E) > |\Delta T_{AD}|^{OFF}(T, E)$ and the paraelectric phase $|\Delta T_{AD}|^{ON}(T, E) < |\Delta T_{AD}|^{OFF}(T, E)$ (Figs. 4b, 5b, and 6b).

3. Study of the ECE in a periodic electric field under quasi-isothermal conditions revealed the significant effect of the pulse profile and frequency on the temperature difference between the thermostated (T_{bot}) and free (T_{top}) ends of the EC element. A decrease in the field frequency leads to an increase in the value of $T_{bot} - T_{top}$, as was observed under the conditions of much lower vacuum [17]. However, this frequency dependence of the cooling deepness is opposite to the dependence expected in the calculations from [15, 16]. One may assume that this difference is most likely related to repolarization and rearrangement of the domain structure of the TGS crystal. Probably, with increasing frequency, the crystal has no time to repolarize/depolarize and, as a result, the ECE value proportional to $\partial P/\partial T$ significantly decreases.

Thus, it is obvious that applying an ac electric field to the EC element under the nonequilibrium thermodynamic conditions related to the fixed temperature of one of the ends makes it possible to implement the temperature gradient along the EC element. The experimentally determined small differences $T_{top} - T_{bot}$ do not allow us to speak about significant heat fluxes between the free and thermostated ends of the EC element, at least in the TGS ferroelectric. However, taking into account that all the data were obtained in the low-strength fields, further investigations of the materials with the more significant ECE in stronger fields are interesting and promising. The most attractive aspect of such studies is the hypothetic possibility of implementation of cooling systems that do not require heat switches.

In view of the aforementioned, we believe that the modified model of a cooled line proposed in [15, 16], in which the repolarization and conductivity effects are taken into account, is of great interest.

ACKNOWLEDGEMENTS

The reported study was funded by Russian Foundation for Basic Research, Government of Krasnoyarsk Territory, Krasnoyarsk Region Science and Technology Support Fund to the research, project no. 16-42-240428 r_a.

REFERENCES

1. M. Tishin and Y. Spichkin, *The Magnetocaloric Effect and Its Application* (Institute of Physics, Bristol, Philadelphia, 2003).
2. K. A. Gschneidner, Jr., V. K. Pecharsky, and A. O. Tsokol, Rep. Prog. Phys. **68**, 1479 (2005).
3. J. F. Scott, Annu. Rev. Mater. Res. **41**, 229 (2011).
4. M. Valant, Prog. Mater. Sci. **57**, 980 (2012).
5. A. Smith, C. R. H. Bahl, R. Bjørk, K. Engelbrecht, K. K. Nielsen, and N. Pryds, Adv. Energy Mater. **2**, 1288 (2012).
6. S. Crossley, N. D. Mathur, and X. Moya, AIP Adv. **7**, 067153 (2015).
7. X. Moya, S. Kar-Narayan, and N. D. Mathur, Nat. Mater. **13**, 439 (2014).
8. I. N. Flerov, E. A. Mikhaleva, M. V. Gorev, and A. V. Kartashev, Phys. Solid State **57** (3), 429 (2015).
9. B. Asbani, J.-L. Dellis, A. Lahmar, M. Courty, M. Amjoud, Y. Gagou, K. Djellab, D. Mezzane, Z. Kutnjak, and M. El. Marssi, Appl. Phys. Lett. **106**, 042902 (2015).
10. H. Liu and X. Yang, AIP Adv. **5**, 117134 (2015).
11. H. Y. Lee, K. H. Cho, and H.-D. Nam, Ferroelectrics **334**, 165 (2006).
12. A. S. Mischenko, Q. Zhang, J. F. Scott, R. W. Whatmore, and N. D. Mathur, Science (Washington) **311**, 1270 (2006).
13. A. S. Mischenko, Q. Zhang, J. F. Scott, R. W. Whatmore, and N. D. Mathur, Appl. Phys. Lett. **89**, 242912 (2006).
14. A. S. Starkov, S. F. Karmanenko, O. V. Pakhomov, A. V. Es'kov, D. Semikin, and J. Hagberg, Phys. Solid State **51** (7), 1510 (2009).
15. I. Starkov and A. Starkov, Ferroelectrics **480**, 102 (2015).
16. A. V. Es'kov, S. F. Karmanenko, O. V. Pakhomov, and A. S. Starkov, Phys. Solid State **51** (8), 1574 (2009).
17. V. S. Bondarev, E. A. Mikhaleva, M. V. Gorev, and I. N. Flerov, Phys. Status Solidi B **253**, 2073 (2016).
18. A. V. Kartashev, I. N. Flerov, N. V. Volkov, and K. A. Sablina, Phys. Solid State **50** (11), 2115 (2008).
19. S. A. Taraskin, B. A. Strukov, and V. A. Meleshina, Sov. Phys. Solid State **12** (5), 1089 (1970).
20. E. F. Dudnik, V. M. Duda, and A. I. Kushnarev, Phys. Solid State **42** (1), 139 (2000).
21. Y. Liu, J. F. Scott, and B. Dkhil, Appl. Phys. Rev. **3**, 031102 (2016).
22. L. D. Landau and E. M. Lifshitz, *Course of Theoretical Physics*, Vol. 5: *Statistical Physics, Part 1* (Nauka, Moscow, 1964; Butterworth–Heinemann, Oxford, 1980).
23. L. Tocado, E. Palacios, and R. Burriel, J. Magn. Magn. Mater. **290–291**, 719 (2005).
24. B. A. Strukov, Sov. Phys. Crystallogr. **11** (6), 757 (1966).
25. Y. Bai, G.-P. Zheng, and S.-Q. Shi, J. Appl. Phys. **108**, 104102 (2010).

Translated by E. Bondareva